

CONFIDENTIAL



#2

V393  
.R463

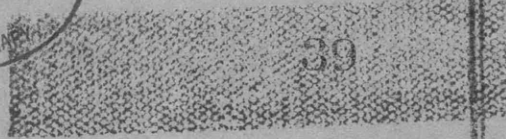
NAVY DEPARTMENT  
THE DAVID W. TAYLOR MODEL BASIN  
Washington 7, D. C.

DYNAMIC LOADING OF A MOTOR TORPEDO BOAT (YP110)  
DURING HIGH-SPEED OPERATION IN ROUGH WATER

BY NORMAN H. JASPER



NS 715-007



CLASSIFICATION CHANGED TO  
*Unclassified*  
IN ACCORDANCE WITH  
*Bushnell Act (P-110)*  
*(526) 526-1297*  
1st *P. Jasper*  
DATE *21 Jul 57*

CONFIDENTIAL

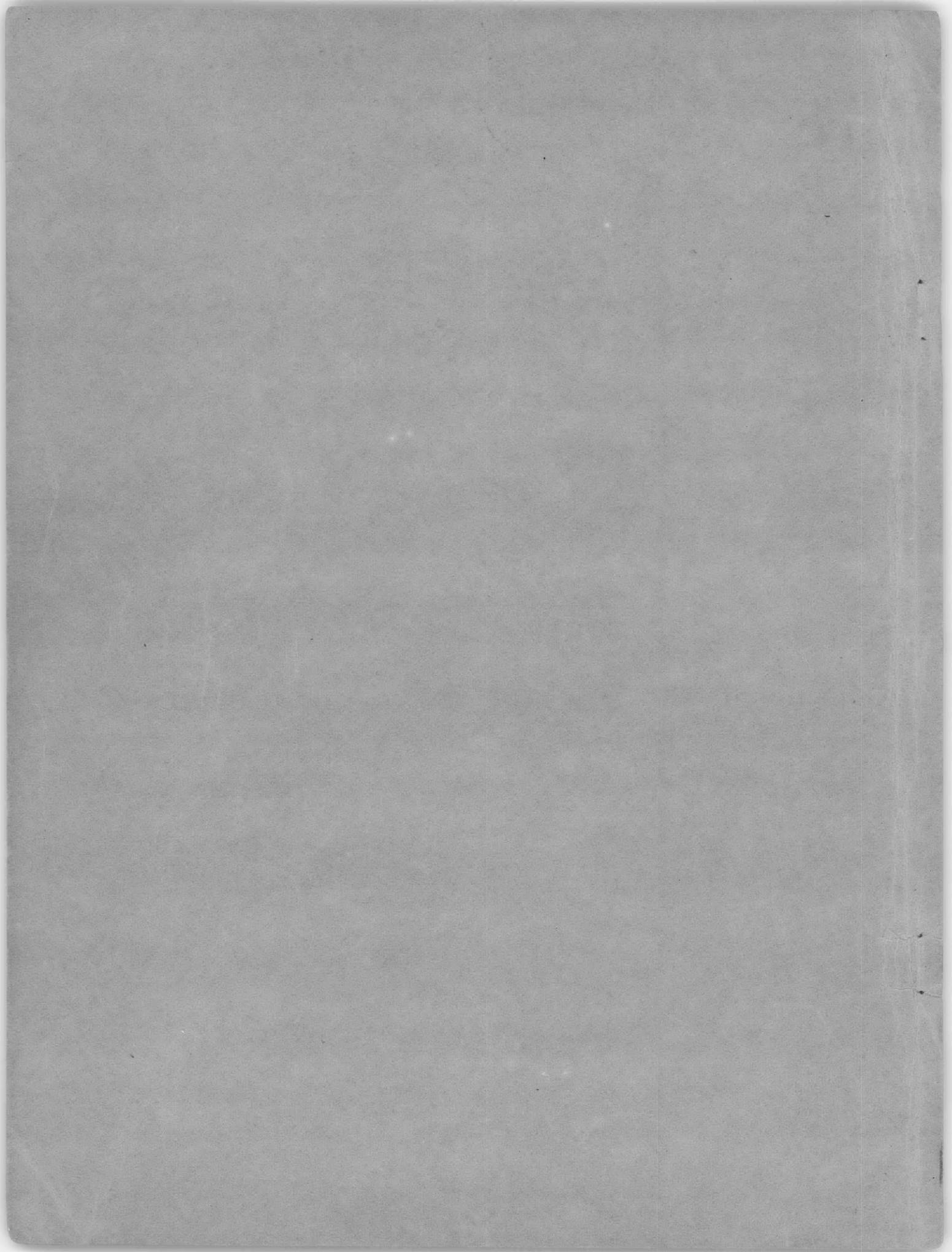
"This document contains information affecting the national security of the United States within the meaning of the Espionage Act, 50 U.S.C., 31 and 32, as amended. Its transmission or the revelation of its contents in any manner to an unauthorized person is prohibited by law."

"Reproduction of this matter in any form by other than naval activities is not authorized except by specific approval of the Secretary of the Navy."

SEPTEMBER 1949

REPORT C-175

CONFIDENTIAL



INITIAL DISTRIBUTION

## Serial

- 1-14 Chief, BuShips, Project Records (Code 362), for distribution:  
1-3 Project Records (Code 362)  
4 Technical Ass't to Chief of the BuShips (Code 106)  
5 Research Division (Code 330)  
6-7 Preliminary Design and Ship Protection (Code 420)  
8 Noise, Shock and Vibration (Code 371)  
9 Hull Design (Code 440)  
10 Scientific (Code 442)  
11 Design Specifications (Code 451).  
12-13 Patrol, District and Minecraft (Code 516)  
14 Coordination of Research and Development (Code 911)
- 15-16 Chief of Naval Research, c/o Navy Research Section,  
Library of Congress, Washington, D.C.
- 17 Director, Naval Research Laboratory, Washington 20, D.C.
- 18 Commander, Naval Ordnance Laboratory, Silver Spring, Md.

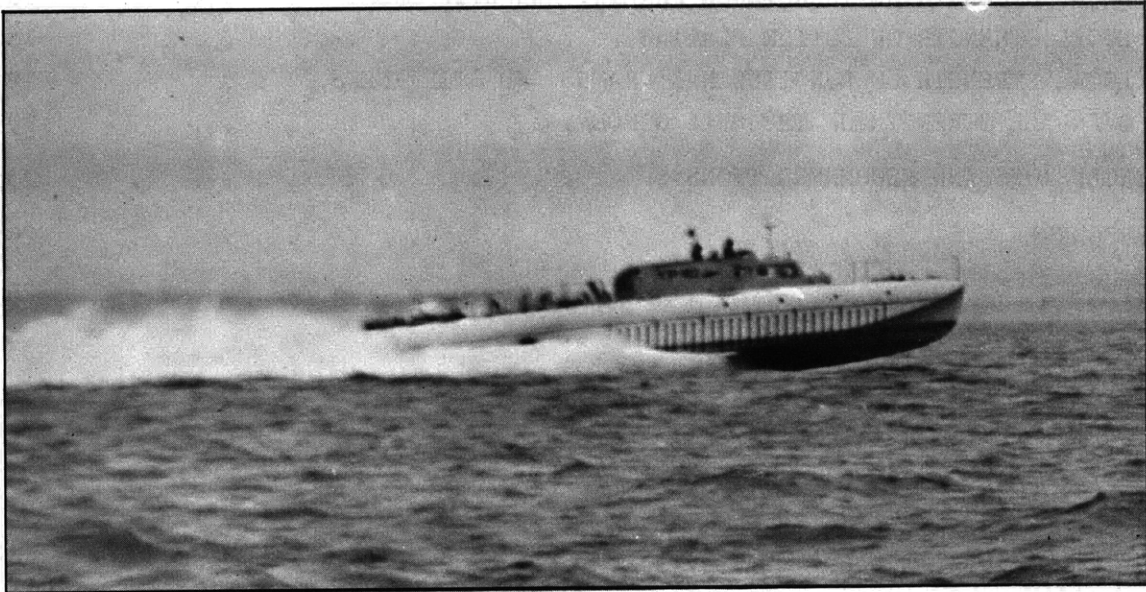




## TABLE OF CONTENTS

	Page
ABSTRACT. . . . .	1
INTRODUCTION. . . . .	1
GENERAL CONSIDERATIONS. . . . .	2
INSTRUMENTATION . . . . .	7
TEST PROCEDURE. . . . .	11
EVALUATION OF DATA. . . . .	12
RECOMMENDED DESIGN PROCEDURES . . . . .	17
LOCAL STRENGTH OF TRANSVERSE FRAMING AND STIFFENERS . . . . .	18
LOCAL STRENGTH OF BOTTOM PLATING. . . . .	18
LOCAL STRENGTH OF LONGITUDINAL FRAMES AND STIFFENERS. . . . .	19
OVER-ALL STRENGTH OF THE HULL GIRDER. . . . .	19
CONCLUSIONS AND RECOMMENDATIONS . . . . .	23
PERSONNEL . . . . .	24
APPENDIX. . . . .	25
REFERENCES. . . . .	33

CONFIDENTIAL



YP110 (Ex PT8)

CONFIDENTIAL

DYNAMIC LOADING OF A MOTOR TORPEDO BOAT (YP110)  
DURING HIGH-SPEED OPERATION IN ROUGH WATER

by

Norman H. Jasper

ABSTRACT

Pressures and strains were measured on the hull of a motor torpedo boat (YP110, Ex PT8) during rough-water operation in order to establish design criteria for hull plating and local structure. The most severe loading due to wave forces occurred between the forward quarterpoint and the midship section. The highest maximum effective pressure for this boat was 36 psi. In order to determine the effective pressures the solution is given for the damped response of a single-degree-of-freedom system to a modified blast pulse.

Failure of portions of the hull structure during these tests indicated that previous design specifications were inadequate. In this report are proposed criteria for designing structures of sufficient local and over-all strength to withstand severe dynamic loading of the type encountered in rough water. Recommendations for further research are made.

INTRODUCTION

The Bureau of Ships directed<sup>1</sup> the David Taylor Model Basin to determine the hydrodynamic loads acting on various parts of an aluminum-hull motor torpedo boat (YP110, Ex PT8) under rough-water conditions. The data were needed in order to establish more realistic criteria for designing the hull plating and framing of a planing boat capable of withstanding the intense loading caused by the impact forces in a rough sea. Secondary aims were to correlate the loading and the resultant stresses in frames and plates as well as to obtain data regarding the load distribution on the hull girders during the rough-water trials.

The YP110 has a displacement of 109,000 pounds, a load waterline length of 75 feet, a beam of 15 feet, and a draft of 3 feet 2 3/8 inches. The moment of inertia of the midship section is 316,800 inches<sup>4</sup>; the effective area of the midship section is 140 square inches.

The tests were made in the roughest water and at the highest speed that was considered safe by the personnel operating the boat. The trials were run in Chesapeake Bay off Norfolk, Virginia, on 9, 13, and 23 January 1948 in waves from 4 to 6 feet in height with a length-to-height ratio of

---

<sup>1</sup>All references are listed on page 33.

about 20--unusually severe conditions for the vessel, the instrumentation, and the test personnel. It is believed that no similar full-scale tests had been conducted previously.

In the present report the pressures due to the dynamic loading are presented in terms of an equivalent static pressure which would produce approximately the same strains as those caused by the dynamic load. The instantaneous transverse-load distribution for a number of instants has been determined at several transverse sections. On the basis of these data, transverse-load-distribution factors were calculated. A method for determining load-distribution factors is recommended. Based on the information available to date, a procedure is presented for determining the equivalent static design load for the local structure, as well as for over-all design of the hull, as required to enable the craft to withstand the severe impacts imposed by rough-water operation. In this connection the equations for the response of a damped single-degree-of-freedom system to a modified blast pulse have been derived.

A preliminary report of these tests was made by TMB CONFIDENTIAL Report C-96.<sup>2</sup>

#### GENERAL CONSIDERATIONS

This section will provide some background information on the type of loading experienced by the bottom structure of a planing boat when it comes in contact with a wave. The concept of equivalent static load and the term "~~shock~~ factor" will be presented. It will be seen that the design of structures to withstand dynamic loads can be considerably simplified by the application of these concepts.

As the boat planes over a wave with zero angle of heading to the waves, the point of initial impact occurs at the keel and at a longitudinal location depending on the relative geometrical configuration of the bottom and the wave. The impact travels aft, and the impact area increases as more of the bottom is wetted. The maximum impact force on the boat is attained after the initial impact. The bottom of PT boats is essentially wedge-shaped. The impact force, per unit of length, acting on a wedge is given by the "virtual mass" impact theory of von Kármán.<sup>3</sup> The transverse distribution of this impact force was measured in the tests which are herein reported. Typical time variations of the impact force are illustrated in the sample record, Figure 1. A simplified illustration of the impact-load variation is shown in Figure 2.

The reaction of a structure to an impact load is, of course, different from that due to the application of a static load. Methods for analyzing

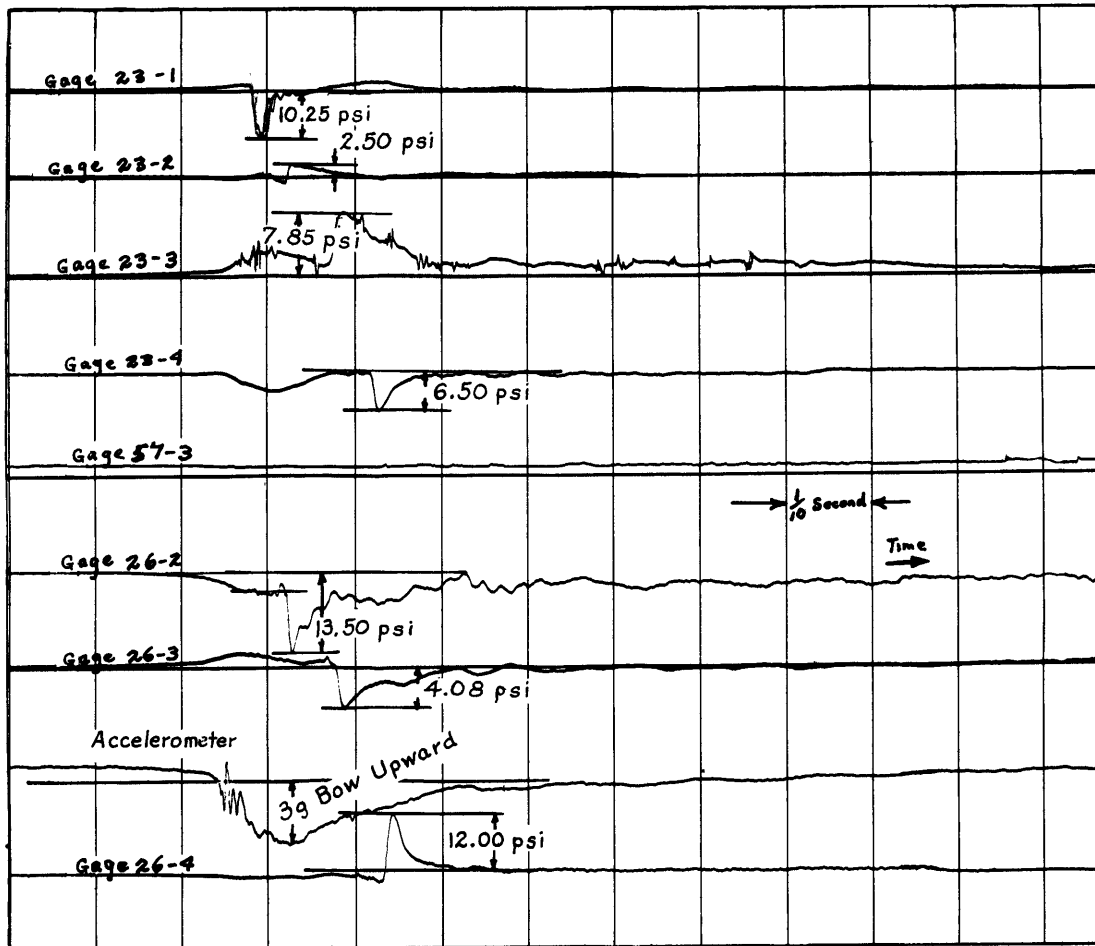


Figure 1 - Pressures Recorded in 5- and 6-Foot Waves  
at a Speed of 28 Knots

these reactions have been well presented by Frankland.<sup>4</sup> In order to simplify the theoretical analysis of the behavior of a structure under impact load, it is assumed that the structure can be idealized as a system with a single degree of freedom. The load acting on this system can be expressed as the non-dimensional ratio of the applied force at any instant to the maximum value of this force; this ratio is called the "disturbance." The ratio of the strain in the system due to the dynamic application of a load  $P$  to the strain due to the static application of the same load  $P$  is termed the "response factor." The numerical maximum value of the response factor is called the "dynamic-load factor." Within the proportional limit, the dynamic-load factor represents the ratio of the static load to the peak dynamic load for the same strain. We may, therefore, obtain an equivalent static load by multiplying the dynamic load by the corresponding dynamic-load factor. Dynamic-load factors were calculated for the impacts measured in these tests.



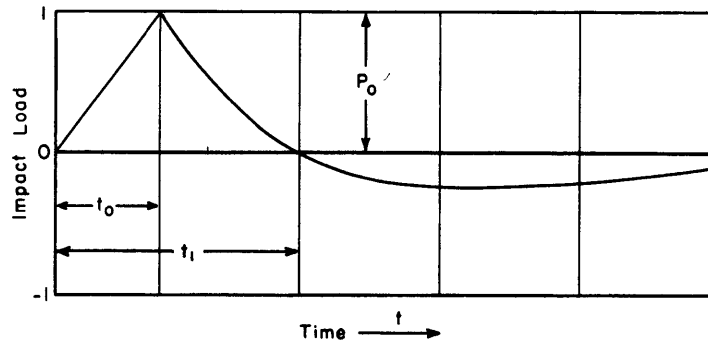


Figure 2 - Typical Time Variation of Impact Load

The peak pressure due to any particular wave impact, when multiplied by the corresponding dynamic-load factor, will give an equivalent static pressure which, if applied to the single-degree-of-freedom system, will result in approximately the same maximum deflection and the same peak stress as are produced by the actual loading. The spatial pattern of pressure distribution is assumed to be fixed, while the actual values of pressure vary with time. This assumption is justified on the basis of the experimental time-space variation of pressure. Damping, which is present in the actual system, will reduce the value of the dynamic-load factor from that obtained by a calculation in which damping forces are neglected. The effect of damping has been considered in the analysis of the test data. Pressures found in this manner have been designated as effective pressures.

A structure may be treated as a single-degree-of-freedom system if one or the other of the following conditions is satisfied:

(a) The time variation of the load has only a small amount of high-frequency content, that is, the coefficients of the Fourier terms which do not correspond to the fundamental mode are relatively small, and the period of the fundamental mode of vibration is several times that of the next higher mode.

(b) The impact load is proportional to  $\int \rho \omega^2 Y(s) ds$ , where  $\rho$  denotes the mass distribution,  $Y(s)$  is the normal mode function,  $s$  is the spatial coordinate, and  $\omega$  is the circular frequency. This requirement is based on the fact that if the space distribution of load, in a linear system, satisfies one of the normal mode functions then no other mode can be excited due to the orthogonality of the normal modes.

The space distribution of the load on the panels and framing, see the Appendix, does satisfy requirement (b) fairly well. The records of the pressure-time variations show but a relatively small amount of high-frequency content.

An approximation of the impact-load variation which generally occurred at the location where the pressures were measured in this series of tests is illustrated in Figure 2.

The differential equation for the response of a single-degree-of-freedom system to this load is

$$\ddot{x} + 2p \frac{c}{c_c} \dot{x} + p^2 x = F(t)$$

where

$$F(t) = \frac{P_0}{m} \frac{t}{t_0} \text{ for } 0 \leq t \leq t_0$$

and

$$F(t) = \frac{P_0}{m} e^{-\frac{t-t_0}{t_1-t_0}} \left[ 1 - \frac{t-t_0}{t_1-t_0} \right] \text{ for } t \geq t_0$$

The solution of the differential equation yields the following:

For  $0 \leq t \leq t_0$

$$u = \frac{x}{\frac{P_0}{mp^2}} = e^{-p \frac{c}{c_c} t} \left[ \frac{\left[ 2 \left( \frac{c}{c_c} \right)^2 - 1 \right]}{pt_0 \sqrt{1 - \left( \frac{c}{c_c} \right)^2}} \sin p \sqrt{1 - \left( \frac{c}{c_c} \right)^2} t + \frac{2 \frac{c}{c_c}}{pt_0} \cos p \sqrt{1 - \left( \frac{c}{c_c} \right)^2} t \right] + \frac{1}{pt_0} \left( pt - 2 \frac{c}{c_c} \right)$$

For  $\infty > t > t_0$

$$u = \frac{x}{\frac{P_0}{mp^2}} = p^2 e^{-p \frac{c}{c_c} t} \left\{ \frac{\left[ 2 \left( \frac{c}{c_c} \right)^2 - 1 \right]}{p^2 t_0 \omega_n} - e^{p \frac{c}{c_c} t_0} \left( \left\{ \frac{\alpha^2 (p^2 \alpha^2 - 1)}{(p^2 \alpha^2 - 2 p \frac{c}{c_c} \alpha + 1)^2} - \frac{pt_0 - 2 \frac{c}{c_c}}{p^3 t_0} \right\} \sin \omega_n t_0 + \left\{ \frac{p \alpha^2 \left( p^2 \alpha^2 \frac{c}{c_c} + \frac{c}{c_c} - 2 \alpha p \right)}{\omega_n (p^2 \alpha^2 - 2 p \frac{c}{c_c} \alpha + 1)^2} - \frac{\frac{c}{c_c} (pt_0 - 2 \frac{c}{c_c}) + 1}{\omega_n p^2 t_0} \right\} \cos \omega_n t_0 \right) \right\} \sin \omega_n t$$

$$\begin{aligned}
& + \left[ \frac{2 \frac{c}{c_c}}{p^3 t_0} + e^{-p \frac{c}{c_c} t_0} \left( \left\{ \frac{p \alpha^2 (p^2 \alpha^2 \frac{c}{c_c} + \frac{c}{c_c} - 2 \alpha p)}{\omega_n (p^2 \alpha^2 - 2 p \frac{c}{c_c} \alpha + 1)^2} \right. \right. \right. \\
& \left. \left. \left. - \frac{\frac{c}{c_c} (p t_0 - 2 \frac{c}{c_c}) + 1}{\omega_n p^2 t_0} \right\} \sin \omega_n t_0 - \left\{ \frac{\alpha^2 (p^2 \alpha^2 - 1)}{(p^2 \alpha^2 - 2 p \frac{c}{c_c} \alpha + 1)^2} \right. \right. \right. \\
& \left. \left. \left. - \frac{p t_0 - 2 \frac{c}{c_c}}{p^3 t_0} \right\} \cos \omega_n t_0 \right) \right] \cos \omega_n t \\
& + \frac{p^2 \alpha^2 e^{-\frac{t-t_0}{t_1-t_0}}}{p^2 \alpha^2 - 2 p \frac{c}{c_c} \alpha + 1} \left( \frac{p^2 \alpha^2 - 1}{p^2 \alpha^2 - 2 p \frac{c}{c_c} \alpha + 1} - \frac{t - t_0}{\alpha} \right)
\end{aligned}$$

where  $t$  is the time,

$t_0$ ,  $t_1$ , and  $P_0$  are defined in Figure 2,

$c/c_c$  is the fraction of critical damping to which the system is subjected,

$p$  is the undamped natural circular frequency of the system,

$\alpha = t_1 - t_0$ ,

$\omega_n = p \sqrt{1 - (c/c_c)^2}$ ,

$u$  is the dynamic-load factor or maximum-response factor, and

$m$  is the mass of the system.

The dynamic-load factor as a function of the ratio of  $t_0$  to the natural period  $T$  of the system is plotted in Figure 3 for three values of damping. This plot covers the range of conditions encountered in the full-scale PT-boat test. The frames and plating of the PT-boat structure were subjected to about 9 percent critical damping when the boat was waterborne. This value of damping reduced the dynamic-load factor by 10 percent. Similar plots of the dynamic-load factors are given by Frankland;<sup>4</sup> however, damping is neglected in his calculations.

It is to be noted that in order to obtain the total effective static pressure at any gage location it is necessary that the hydrostatic pressure acting at that gage location, when the vessel is at rest, be added to the effective pressures given in this report. This is due to the fact that the gages measure the variation of the pressure from the hydrostatic pressure with the boat at rest. The total effective static pressures as

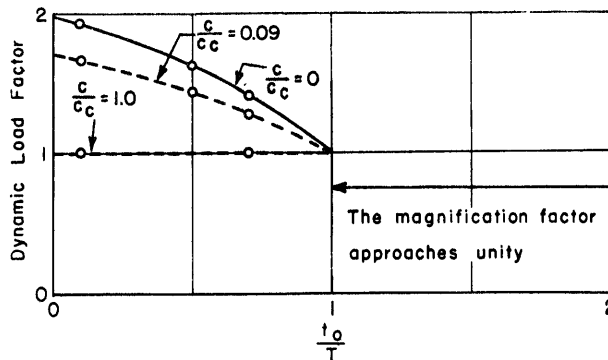


Figure 3 - Dynamic-Load Factors for Impacts  
of the Type Illustrated by Figure 2

$$t_1 = 10T$$

defined above may be used as equivalent static load in designing the shell plating and framing, which can be considered as single-degree-of-freedom systems.

#### INSTRUMENTATION

Since the primary object of the test was to determine the local loading of frames and of plating panels, and since it was expected that the instantaneous impact loads would be concentrated in a relatively short transverse section of the ship, it was decided to arrange the instrumentation in transverse belts. This would permit simultaneous recording of pressures and strains. The hull is, of course, symmetrical with respect to the longitudinal centerline plane, and it was assumed that measurements made on one side of the hull would also be representative of those on the other side. Thus only the starboard side of the vessel was instrumented. Since the instrumentation was to be subjected to rather severe shock and vibration, the electrical instruments were supplemented with mechanical gages. Photographs of the installation are shown in Figure 4.

Preliminary test runs had shown the necessity of shock-mounting the amplifying equipment to withstand the severe impacts--which occurred on the hull at frequencies of about 3 cps or less. Electronic equipment (for SR-4 strain gages and for diaphragm-type pressure gages) was accordingly mounted in a rack made of angle irons, and the entire rack was then supported by B.F. Goodrich Type-10 rubber mounts, giving a natural frequency of 7.2 cps in the vertical direction. The support was to provide shock protection; it was not intended to be a vibration isolation mount. The shock loads in the longitudinal and athwartships direction were relatively minor. This shock mounting performed satisfactorily throughout the tests.

The instrumentation comprised TMB diaphragm-type pressure gages, De Juhasz engine indicators modified to record the maximum value of the relatively small hydrodynamic pressures, SR-4 strain gages, DeForest scratch-recording strain gages, Statham accelerometers, and Jacklin accelerometers measuring linear and angular accelerations of the hull. The pressure and strain gages, the outputs of which were to be recorded oscillographically, were arranged in seven transverse belts. The belts or groups were spaced at intervals of from 3 to 7 frame spaces. A five-digit number was assigned to each gage--the first two digits indicated the number of the frame forward of the gage, the third digit the relative position of the gage in its belt from the keel outboard, and the last two digits the oscillograph channel on which the signal was recorded. In designating the gages in this report, the last two digits have been omitted. The gages were connected to eight separate 3-point multiposition switches, on each of which nine positions were used. To record the data from any one of the seven groups of gages, it was only necessary to turn each switch to the position corresponding to the desired gage group. Thus to record the output of group six, all switches were set to number six. The output of the Statham accelerometer was recorded with every group.

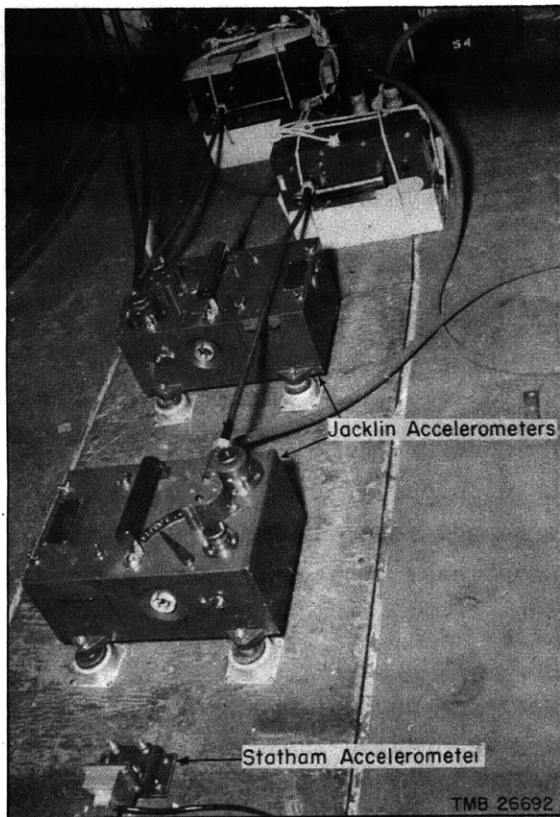


Figure 4a - Installation of Accelerometers

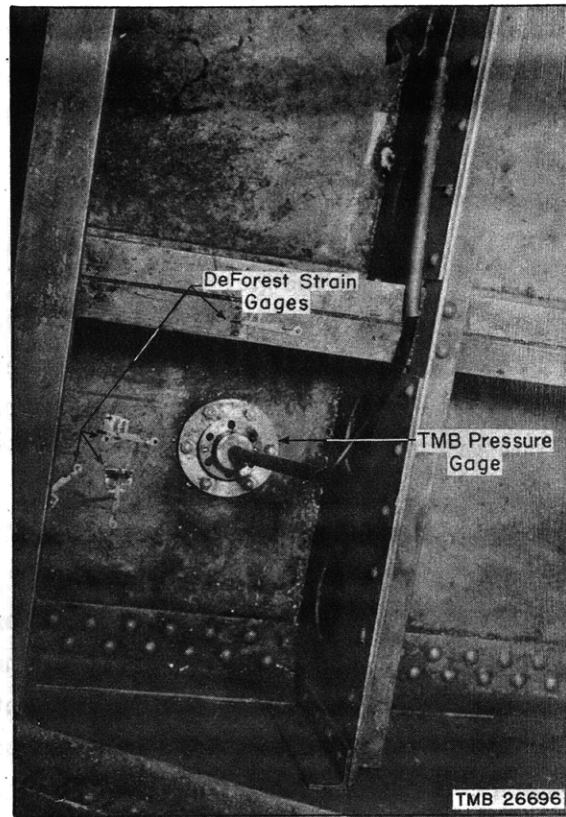


Figure 4b - Installation of Diaphragm Pressure Gage and DeForest Strain Gages



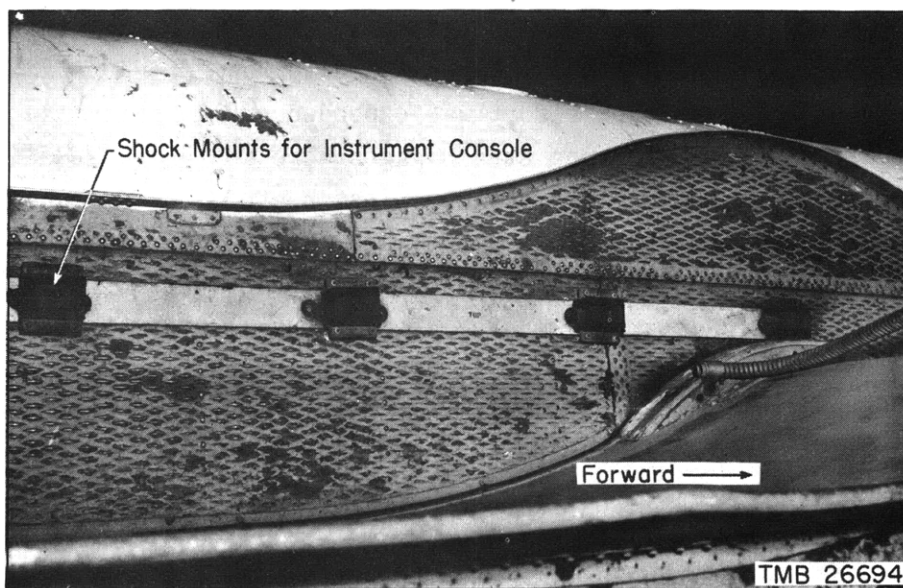


Figure 4c - View of Shock-Mount Installation, Looking Down on Main Deck



Figure 4d - Shock-Mounted Console

Figure 4 - Installation of Instruments and Equipment on YP110

The modified De Juhasz engine indicator did not perform satisfactorily, primarily because the indicator stylus tore through the paper, and the gage operated sluggishly. Since the diaphragm pressure gages gave satisfactory data, no further effort was expended on improving the mechanical gage. Type SR-4 wire-resistance strain gages were installed at several locations. The cleaned aluminum surface was first heated, the gage was then cemented to the surface with Duco cement, and, after the cement had dried, both the gage and the lead wires were covered with beeswax. DeForest scratch-type strain gages were mounted at numerous locations both singly and in rosette patterns; see Figure 4. Although these gages were intended to furnish only the peak strain in any given test, it was thought possible to determine the associated peak stress--under the not unreasonable assumption that at any given location the peak strains would occur simultaneously along the several directions. A Statham accelerometer, rated at  $\pm 10$  g, was shock-mounted at the centerline near the forward quarterpoint and oriented to record vertical accelerations; see Figure 4. The Jacklin angular and linear accelerometers were installed as shown in Figure 4 and operated by remote control from the bridge. A detailed description of this instrument is given in an earlier TMB report.<sup>5</sup> Unfortunately the Jacklin accelerometers did not operate satisfactorily under the most severe loading conditions.

An aircraft-type accelerometer (BuAer Stock Number NOA(s) 6297) was used to give a rough indication of the maximum accelerations experienced on the bridge. The natural frequency of this accelerometer was 8.75 cps, and its damping was 4 percent of the critical value.

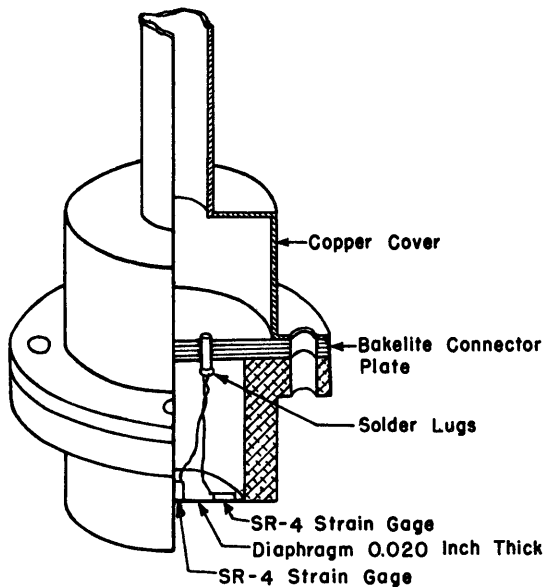


Figure 5 - TMB Diaphragm Pressure Gage

The diaphragm pressure gage was developed at the Taylor Model Basin<sup>6</sup> and is illustrated schematically in Figure 5. When the gage is subjected to external pressure, the aluminum diaphragm is deformed elastically, owing to the unbalance in pressures acting on the outer and inner surfaces. The elastic strains in the clamped diaphragm developed by this action cause corresponding resistance variations in the strain gages which are cemented to the diaphragm. To ensure linear gage response the usable range is selected so as to limit the

diaphragm deflections to one-third the thickness of the diaphragm.

The entire gage cup was machined out of 61ST duralumin. The output of the gage is temperature-compensated. The SR-4 strain gage and its lead wires were covered with a thin coat of beeswax; the body of the gage was then filled with Vaseline. The gages were attached to the inboard side of the shell plating, with the gage cup projecting through a hole and the diaphragm flush with the outside of the plating. A two-conductor shielded rubber cable connected the gages to the multiposition switches in the instrument room. The signals from the strain and pressure gages were amplified by TMB Type 1A strain indicators which had given satisfactory service in previous tests. This standardized strain indicator (described in TMB Report 565<sup>7</sup>) is intended to be used with SR-4 strain gages of 120-ohm resistance.

Before concluding the subject of instrumentation it should be added that motion pictures of the YP110 were made from another PT boat during part of the rough-water trials.

#### TEST PROCEDURE

Before the test runs were conducted, the electronic equipment was allowed to warm up to operating temperature. Some attempt was made to keep the instrument room at an even temperature in order to minimize temperature effects on the equipment. The strain indicators were then balanced against a dummy strain gage against which, in turn, the active gages had previously been balanced. Calibration signals were then imposed on each strain indicator and recorded on the oscillograph. The instrument room was manned by two operators who could communicate by telephone with the bridge. One man operated the multiposition switches, and the other operated the oscillograph. The oscillograph operator was strapped to his seat to prevent being thrown against the overhead by the intense shocks. The boat was headed into the waves at shaft speeds ranging from 1400 engine rpm (corresponding to about 24 knots) to 2000 engine rpm (corresponding to approximately 35 knots). During each run a constant speed was maintained while the pressures, strains, and accelerations were measured for the most significant gage groups. The most severe condition was selected by visual inspection of the signals, and the boat was then operated at the speed for this condition with various angles of heading to the waves.

From the tests it was found that the most severe shocks were encountered with approximately zero angle of heading at the highest speed which was considered safe for both crew and ship. At this speed of 35 knots and zero angle of heading, the output of several gage groups was

recorded, one group at a time, together with the acceleration peaks indicated by the BuAer accelerometer on the bridge.

Although preparations for making rough-water measurements were rehearsed many times, considerable time passed before suitable rough weather materialized. During this interval a number of pressure and strain gages were replaced because of mechanical or electrical failure. The salty, humid atmosphere, together with the intense pounding to which the equipment was subjected during the trials, made unusual demands on both personnel and equipment.

EVALUATION OF DATA

The data were analyzed with the objective of obtaining equivalent static design loads which could be applied to the design of local structure. The full-scale test data as well as model-test data<sup>8</sup> were then evaluated so as to provide a procedure for the over-all strength design of the ship girder. The pressures due to the impact loads acting on the hull were evaluated in terms of effective pressures according to the method outlined under "General Considerations." The effect of damping was considered.

Figures 6 and 7 show the magnitudes of effective pressures during two sea conditions. The maximum and the average of at least five relatively

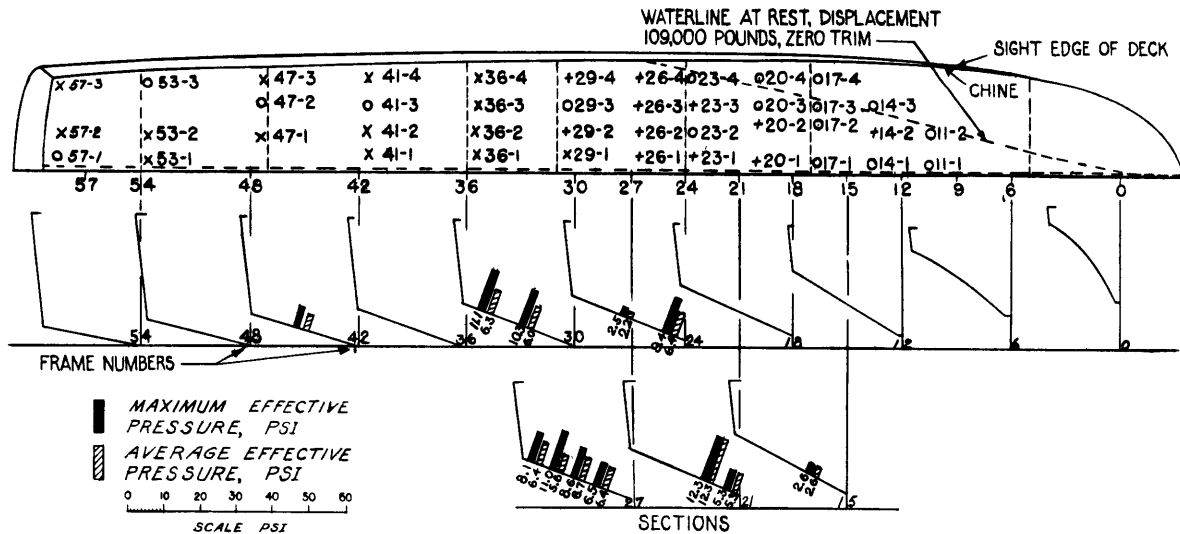


Figure 6 - Distribution of Pressure Along the Bottom in 4- to 5-Foot Waves

Pressures in 4- to 5-foot waves were measured with the vessel operating at 35 knots, corresponding to 2000 engine rpm.

Locations of active gages are designated by "+," followed by the gage number. Gages at locations designated by "x" were out of order or were not used. Gages at locations designated by "o" recorded pressures less than 2 psi.

The average pressures tabulated are averages of five or more measurements.

intense impulses occurring at each gage are shown. Table 1 gives the maximum and average effective pressures as well as the hydrostatic still-water pressures acting at the several gages. The highest maximum effective pressure tabulated is 36 psi. This pressure occurred on the plate between Frame 17 and Frame 18. Table 1 includes several maximum effective pressures between 27 and 36 psi.

The bottom structure of the PT boat was damaged during the tests as a result of the impact loading. Considerable work would have to be accomplished in order to restore the original strength; however, the boat was not incapacitated. The floors buckled in localized areas from amidships to the forward quarterpoint. This damage does, in a qualitative sense, verify the high pressures measured, and it demonstrates the ability of the aluminum hull to deform and absorb energy without appreciable leakage.

Inspection of the pressure data and of the motion pictures taken during the tests indicate that the maximum pressure may occur anywhere from about the forward quarterpoint to amidships. If enough measurements had been made, a maximum effective pressure of 36 psi would probably have occurred at some time at every gage in this impact area. The bow of the boat, due to the relatively sharp dead rise, would probably be subjected to lower pressures than the aforementioned "impact area" even if, on occasion, impact with

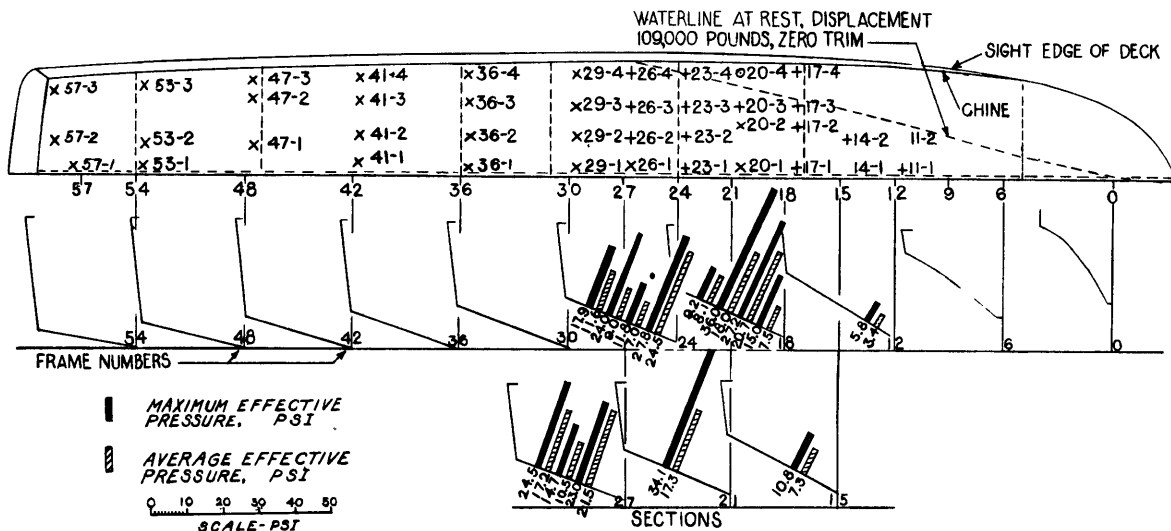


Figure 7 - Distribution of Pressure Along the Bottom in 5- to 6-Foot Waves

Pressures in 5- to 6-foot waves were measured with the vessel operating at speeds from 28 to 35 knots, corresponding to 1600 to 2000 engine rpm.

Locations of active gages are designated by "+," followed by the gage number. Gages at locations designated by "x" were out of order or were not used. Gages at locations designated by "o" recorded pressures less than 2 psi.

The average pressures tabulated are averages of five or more measurements.



TABLE 1

Effective Pressures Measured During Rough-Water Trials of YP110

Gages which were out of order are not listed in this table. Measurements in 4- to 5-foot waves were made with the vessel operating at 35 knots, corresponding to 2000 engine rpm. Measurements in 5- to 6-foot waves were made with the vessel operating at speeds from 28 to 35 knots, corresponding to 1600 to 2000 engine rpm.

The effective pressures have been corrected for the effect of damping. The average pressures tabulated are averages of five or more individual measurements.

Gage Number	Effective Pressure, psi				Hydrostatic Pressure at Gage, Ship at Rest, psi
	4- to 5-Foot Waves		5- to 6-Foot Waves		
	Maximum	Average	Maximum	Average	
11-1	negligible		5.8	3.4	0.9
11-2	negligible		*	*	0.3
14-1	negligible		negligible		1.0
14-2	2.6	2.6	10.8	7.3	0.5
14-3	negligible		negligible		0
17-1	negligible		15.0	7.5	1.1
17-2	negligible		27.2	20.7	0.5
17-3	negligible		36.0	18.0	0.6
17-4	negligible		9.2	8.1	0
20-1	5.3	5.3	*	*	1.2
20-2	12.3	12.3	*	*	0.6
20-3	negligible		34.1	17.3	0.2
20-4	negligible		negligible		0
23-1	9.4	6.4	27.8	24.5	1.3
23-2	negligible		11.8	7.0	0.8
23-3	2.5	2.2	24.0	9.0	0.4
23-4	negligible		17.9	11.6	0
26-1	6.5	6.4	*	*	1.3
26-2	8.6	6.7	23.0	21.5	0.9
26-3	11.0	5.6	14.7	10.5	0.5
26-4	8.1	6.4	24.5	17.2	0.1
29-2	10.3	6.0	*	*	0.9
29-3	negligible		*	*	0.6
29-4	11.1	6.3	*	*	0.2
41-3	5.8	4.7	*	*	0.8
47-2	negligible		*	*	1.2
53-3	negligible		*	*	1.0
57-1	negligible		*	*	1.4

\* No data were obtained.

the water should occur. Based on these considerations an "impact factor" was plotted (see Figure 9a on page 18). The plot may be regarded as the envelope of a series of curves, each curve corresponding to a given combination of speed and sea conditions. The impact factor is intended to be proportional to the probable maximum effective pressure at any point along the boat.

The maximum accelerations measured by the Satham accelerometer at Frame 15 1/2 during operations in 5- to 6-foot waves are tabulated in Table 2, for a number of the more severe impacts. The accelerations measured by

TABLE 2

Peak Accelerations Measured by Satham Accelerometer  
at the Forward Quarterpoint of the YP110  
During Operation in 5- to 6-Foot Waves

Shock No.	Record No.	Peak Acceleration g*	Engine rpm
1	04410	4.5	2000
2	04412	3.0	2000
3	04414	5.0	2000
4	04415	8.0	2000
5	04433		2000
6	04435	3.5	2000
7	04423	3.5	1600
8	04423	2.0	1600
9	04408	3.0	2000
	04403	4.3	1600
	04428	3.0	2000
	04432	4.7	2000
	04418	2.5	1600
	04400	3.0	1600
	04403	2.5	1600
	04409	3.7	2000
	04414	4.5	2000

\*g is the acceleration of gravity.

the BuAer accelerometer on the bridge were of the order of 6 and 7 g; one impact gave a reading of about 12 g. The distribution of acceleration along the hull is given in Figure 10 on page 20 for the most severe shock encountered during the tests. This plot is based on the motion of the boat obtained from motion pictures, the peak accelerations measured with the Satham accelerometer, and a distribution of acceleration similar to that found by model tests carried out by Siler and Anderson in 1947.<sup>8</sup> The rigid-body acceleration is found to vary linearly from about +11 g at the bow to -2 g at the transom.

In order to determine the transverse-load distribution during wave impacts the following analysis was made. The instantaneous transverse-load distribution was plotted for the impact which gave the highest pressure recorded for each gage on Frames 17, 23, and 26. For several other severe shocks the pressure distribution was plotted for the several instants at

which each one of the gages in the particular transverse section reached a maximum. A total of 55 such plots were made; see the Appendix. These load-distribution curves were then used to determine:

- (a) The shape of the transverse-load distribution.
- (b) A transverse-load-distribution factor based on an unsupported width of structure equal to 100 percent, 20 percent, and 0 percent of the breadth from keel to chine. This factor will be discussed in detail later.
- (c) A longitudinal-load-distribution factor. This factor will also be discussed in detail later.

The transverse-load-distribution factor was calculated as follows. An inspection of the typical transverse-load distributions in the Appendix shows that the load which travels over the entire width from keel to chine can be reasonably approximated by a versed sine function. The maximum value of the load is a function of both time and space. The most severe loading of a beam or plate would occur with the pressure peak located at the center of the structure as illustrated in Figure 8. The maximum stress was calculated for a beam of uniform section modulus loaded with a sinusoidal load as shown in Figure 8. The calculation was made for both the pin-ended

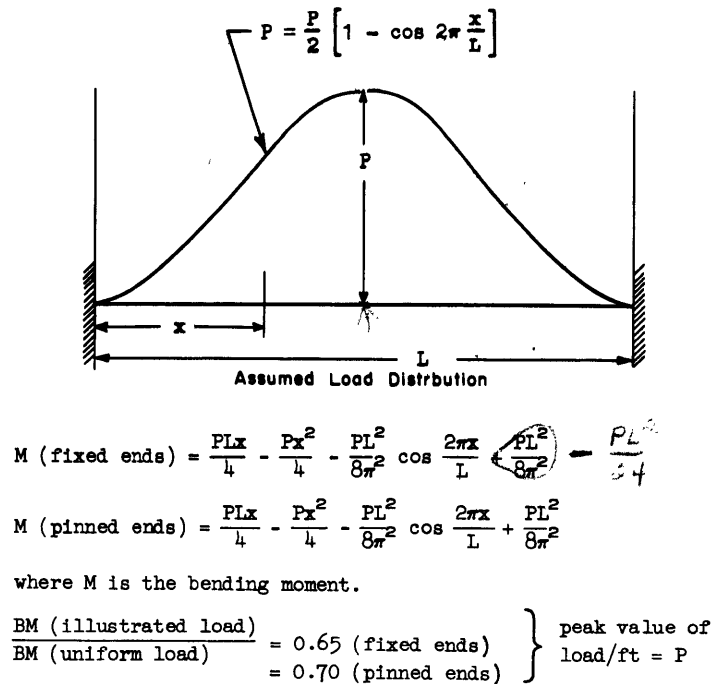


Figure 8 - Typical Transverse-Load Distribution at Instant of Peak Impact Load

and the fixed-ended conditions. For both conditions the uniform load which would give the same deflection as the sinusoidal load was calculated. The ratio of this uniform load to the peak value of the sinusoidal load is termed the transverse-load-distribution factor for a 100 percent unsupported half breadth. The load factor thus calculated is 0.70 for the pin-ended condition and 0.65 for the fixed-ended condition. An average value of 0.68 was selected. Multiplying the peak load at any section by this factor will give an equivalent uniform load which will result in approximately the same maximum stress as the sinusoidal load distribution.

The transverse-load-distribution factor for the 20-percent unsupported width was approximated by determining the maximum value of the ratio of the mean pressure to the maximum pressure in any 20-percent width of the span (see the Appendix). The transverse-load-distribution factors are plotted in Figure 9c.

An assumed longitudinal-pressure distribution over the bottom is plotted in Figure 12 on page 21. This plot is based on model tests and on the impact theory of von Kármán.<sup>3</sup> The pressure load at the bow is made equal to zero so as to agree with the actual observations. It is recommended that for any actual design, longitudinal-load distributions be determined as in the model tests reported by Siler and Anderson.<sup>8</sup>

The longitudinal-load-distribution factor is used to check the local strength of longitudinal structures. Since the peak impact load does not occur simultaneously in the same longitudinal plane for every transverse section, it is believed reasonable to base this factor on the average maximum load occurring at any transverse section. The longitudinal-load-distribution factor, plotted in Figure 9b, is the ratio of the average pressure over the entire span to the maximum pressure determined from the experimental transverse-load distributions.

#### RECOMMENDED DESIGN PROCEDURES

In this section the suggested procedure to be applied in the design of the various types of planing-boat structures are set forth, together with illustrative applications.

In general, each structural part of the boat will have to be designed from considerations of, first, the over-all strength of the hull girder and, second, the local strength of the structure required to withstand the localized impact loads. The more severe of these two requirements will be the one to govern the design.

The structural parts of the hull may be divided into four categories, to each of which a different design procedure will apply. These categories are as follows:

1. Transverse framing and stiffeners.
2. Bottom plating.
3. Longitudinal frames and stiffeners.
4. Structure which contributes to over-all hull girder strength but which is not subjected to localized impact loads.

Local Strength of Transverse Framing and Stiffeners

The loading is determined by applying to the structure a uniform load per unit area (the design load)

$$p = (P \times F_I \times F_T) + P_h$$

where P is the maximum effective pressure (36 psi for the YP110),

$F_T$  is the "transverse-load-distribution factor" from Figure 9c,

$F_I$  is the "impact factor" from Figure 9a, and

$P_h$  is the hydrostatic pressure, with the boat at rest.

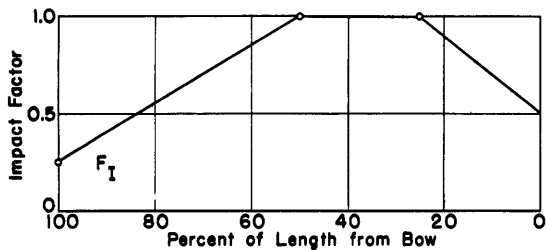


Figure 9a

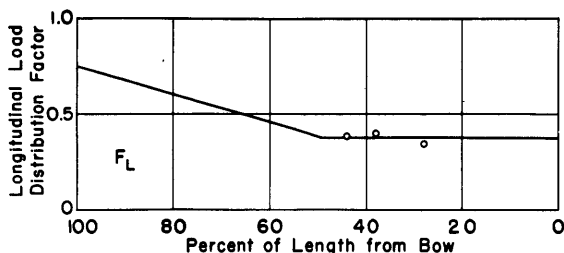


Figure 9b

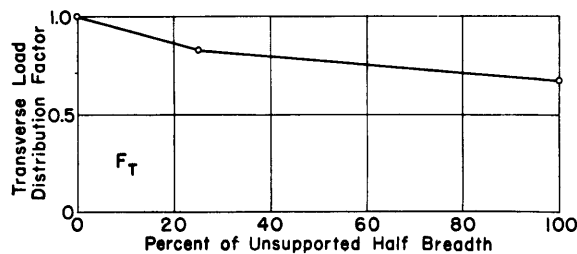


Figure 9c

Figure 9 - Load Factors Used in Design of Local Structures

As an example, assume that it is desired to determine the design load on a frame at a location 0.7 of the length of the boat from the bow. Since 100 percent of the bottom half breadth is supported,  $F_T$  is equal to 0.68 and  $F_I$  is equal to 0.7. The hydrostatic load at the center of the frame is about 0.5 psi. Therefore the design load is

$$p = 36 (0.68)(0.70) + 0.5 = 17.6 \text{ psi}$$

Local Strength of Bottom Plating

The design load for bottom plating is determined in the same manner as that for transverse framing and stiffeners. The selection of minimum satisfactory plating thicknesses to resist normal loading cannot be made by using formulas based on Hooke's law. The selection should be based upon



allowable permanent set. An allowable permanent set of 0.005 times the shortest side is recommended as in a post-war set of BuAer specifications for the rigidity and strength of airplanes.<sup>9</sup>

#### Local Strength of Longitudinal Frames and Stiffeners

The design load is determined by applying a load to the structure which, for any longitudinal location, is

$$p = (P \times F_I \times F_L) + P_h$$

where  $p$  is the load per unit area at the particular longitudinal location under consideration (this value will be independent of the width of plating supported),

$P$  is the maximum effective pressure (36 psi for the YP110),

$F_I$  is the "impact factor" from Figure 9a,

$F_L$  is the "longitudinal load distribution factor" from Figure 9b, and

$P_h$  is the hydrostatic pressure with the boat at rest.

As an example, assume that it is desired to design a longitudinal extending from one-eighth to one-quarter the length of the boat from the bow. The design loads are as follows:

$$P_{\frac{1}{8}l} = (36 \times 0.75 \times 0.38) + 0.5 = 10.8 \text{ psi}$$

$$P_{\frac{1}{4}l} = (36 \times 1.0 \times 0.38) + 0.5 = 14.2 \text{ psi}$$

$$\text{Average value of } P = 12.5 \text{ psi}$$

#### Over-All Strength of the Hull Girder

The shearing forces and bending moments in the hull girder are determined as follows. The hull girder is assumed to act as a rigid body, which is nearly true, and to be subjected to rigid-body accelerations similar to those plotted in Figure 10. These accelerations may be obtained from model tests. Load components in other than the vertical direction are neglected.

Figure 11 is a schematic representation of the hull girder and the forces acting on it. Referring to Figure 11a we may then write the following equation:

$$\int_0^l \frac{W}{g} \ddot{y} \, dx = -V - \int_0^l w \, dx + \int_0^l p \, dx \quad [1]$$

where  $w$  is the weight per unit length at any point  $x$  obtained from the weight curve of Figure 11b,

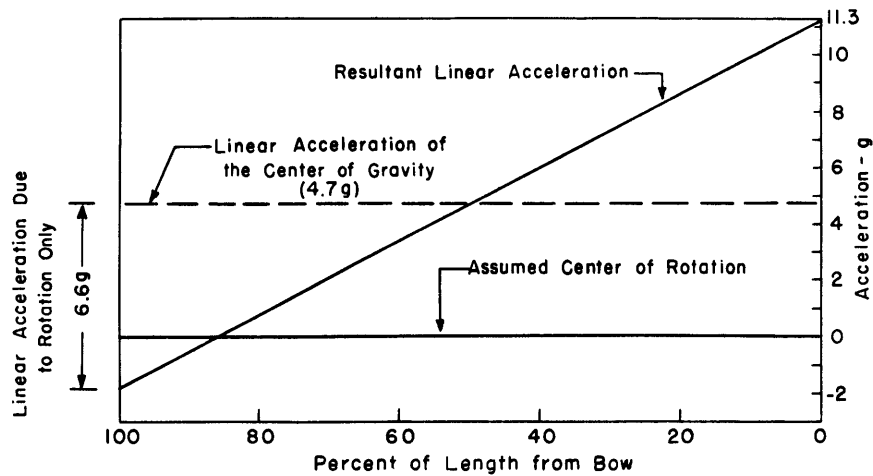


Figure 10 - Distribution of Rigid-Body Acceleration along the Hull at Instant of Greatest Impact Load

$\ddot{y}$  is the vertical component of the resultant linear acceleration at any point  $x$ , obtained from a curve similar to Figure 11c,  
 $p$  is the external load per unit length at any point  $x$ , as obtained from a load curve similar to that given in Figure 11d,  
 $V$  is the shear force acting at  $x = \xi$  on the section of the hull extending from  $x = 0$  to  $x = \xi$ , and  
 $g$  is the acceleration of gravity.

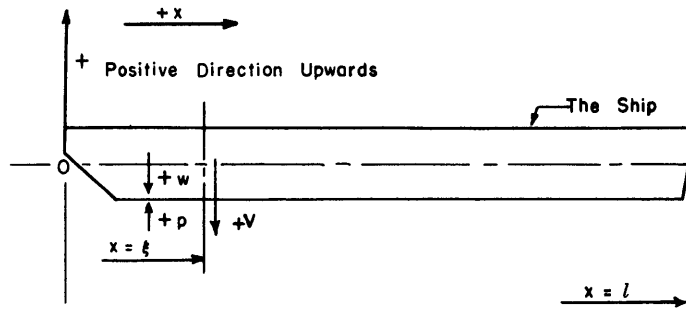
The actual calculation can be carried out in a rather simple manner as follows:

1. Determine and plot a weight curve  $w(x)$ , Figure 11b.
2. Determine and plot the acceleration curve  $\ddot{y}(x)$ , Figure 11c or Figure 10.
3. Determine and plot the external-load curve  $p(x)$ , Figure 11d or Figure 12.
4. To determine the shear  $V$  at any longitudinal location  $x = \xi$ , evaluate by graphical integration the integrals of Equation [1]. The shear is then

$$V = - \int_0^{\xi} \frac{W}{g} \ddot{y} dx - \int_0^{\xi} w dx + \int_0^{\xi} p dx \quad [2]$$

5. The shear curve  $V(x)$  is then plotted and integrated in order to give the bending-moment curve.

$$\int_0^{\xi} \frac{w}{g} \dot{y} \, dx = -V - \int_0^{\xi} w \, dx + \int_0^{\xi} p \, dx \quad \text{Equation [1]}$$



$w$  is the weight per unit length  
 $p$  is the external pressure load per unit length  
 $V$  is the shear force acting on the left of the section  
 $\dot{y}$  is positive upward

Figure 11a

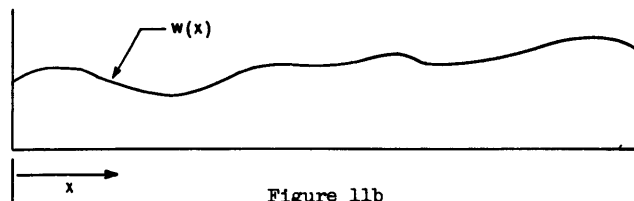


Figure 11b

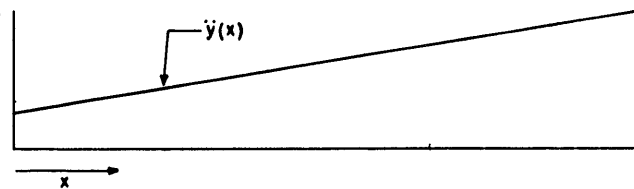


Figure 11c

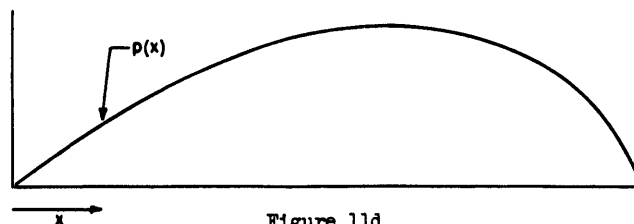


Figure 11d

Figure 11 - Diagrams to Illustrate the Calculation of the Stresses in the Hull Girder

Figures 11b, 11c, and 11d are not intended to bear any resemblance to the actual variations  $w(x)$ ,  $\dot{y}(x)$ , and  $p(x)$ .

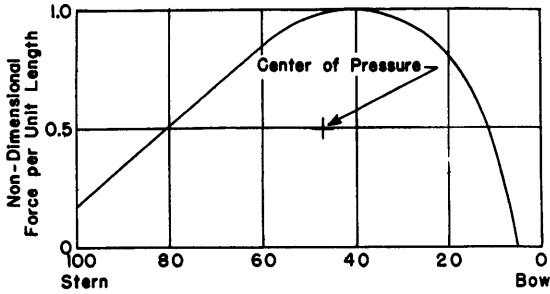


Figure 12 - Longitudinal Distribution of Load Due to Bottom Pressure at Instant of Greatest Impact Load

The area under this curve represents the vertical component of the total pressure load acting on the vessel.

If the actual load curve  $p(x)$  is not available, a spatial pressure load distribution similar to that shown in Figure 12 may be assumed. The area under this curve is

$$\int_0^l p \, dx = \int_0^l \frac{w}{g} \ddot{y} \, dx + \int_0^l w \, dx$$

The longitudinal center of pressure (LCP) of  $p(x)$  can be determined as

$$LCP = \frac{I \ddot{\theta} + \int_0^l wx \, dx}{\int_0^l p \, dx} \quad [3]$$

where

$$I = \int_0^l \frac{w}{g} x^2 \, dx$$

and  $\ddot{\theta}$  is the angular rigid-body acceleration of the boat.

An equivalent procedure, when the design is treated as a problem in statics, is as follows:

1. Plot the weight curve  $w(x)$ .
2. Multiply the weight curve by the respective acceleration curve and plot the product  $w(x) \ddot{y}(x)/g$ .
3. Determine the algebraic sum of 1 and 2,

$$\left[ w(x) + \frac{w(x) \ddot{y}(x)}{g} \right]$$

4. Assume a pressure distribution  $p(x)$  similar to that shown in Figure 12. The area under this pressure curve must equal the load given in Step 3, i.e.,

$$\int_0^l p \, dx = \int_0^l \left[ w(x) + \frac{w(x) \ddot{y}(x)}{g} \right] dx$$

Also the center of pressure must satisfy Equation [3].

5. The resultant equivalent static load per unit length acting at any point  $x = \xi$  is equal to the algebraic difference of Steps 3 and 4, i.e.,

$$\text{Equivalent static load } (x) = - \left[ w(x) + \frac{w(x) \ddot{y}(x)}{g} \right] + p(x)$$

6. The shear and bending moment may be obtained by the integration of the load curve.

It is recommended that the longitudinal load distribution be determined by means of the procedure outlined by Siler and Anderson,<sup>8</sup> which necessitates model tank tests of the proposed design together with the application of the impact theory of von Kármán. In the absence of model tests the load distribution of Figure 11 may be used for the design of boats similar to the YP110.

In view of the more realistic standards of loading proposed in this report it is considered that a safety factor of about 1.1 based on the yield strength is justified for the design of all structural components except plating. Plating should be designed on the basis of an allowable permanent set.

#### CONCLUSIONS AND RECOMMENDATIONS

1. The pressure-time pattern during impact for V-bottom planing craft with normal dead rise is almost invariably of the type illustrated in Figure 2. This conclusion is corroborated by comparable tests of other investigators.<sup>8, 10</sup>

2. The bottom plating panels and the transverse frames may be considered as single-degree-of-freedom systems when it is desired to calculate their response to impact loads of the type measured during the full-scale YP110 trials.

3. The hull frames and panels of the YP110 when loaded by water on one side are subjected to about 9 percent of critical damping. The effect of this damping is to reduce the stresses by about 10 percent.

4. The maximum effective pressure that is likely to be experienced by the YP110 during rough-water trials is 36 psi. This value will, in general, be different for different boats depending on the geometry of the vessel, its speed relative to the waves, sea conditions, and the rigidity of the component structures. The maximum effective pressure appeared to increase with ship's speed and decrease with the angle of heading for the range of speeds covered, that is, up to 35 knots.

5. The framing and hulls of craft of this design should be strengthened if it is desired to ensure against structural damage when operating at high speeds in seas of the magnitude encountered during these tests. It is understood that a static-pressure loading of 10 psi was used in the original design of bottom structure of this craft. On the basis of this report it is evident that this value should be substantially increased. In this

connection, however, it should be borne in mind that any changes in scantlings made solely on the basis of equivalent static pressures may not produce a proportional change in the ability of the structure to withstand peak loads where dynamic loads are involved, in as much as the effect of the structural changes on the natural frequency of vibration, and hence on the dynamic load factor, must also be considered. In the present case it appears that there would be a gain in two different respects through increasing the strength of framing and plating:

(a) The maximum stress would be reduced directly by the increased moment of inertia of the section, and

(b) The dynamic load factor, and hence the equivalent static pressures, would be reduced by the presumably greater rigidity and consequent higher natural frequency of vibration of the structure in question.\*

6. The maximum acceleration to be anticipated on this type of craft at the quarterpoint is of the order of 8 g.

7. The damage suffered by the YP110 during the rough-water tests does, in a qualitative sense, verify the high pressures measured, and it demonstrates the ability of the aluminum hull to deform and absorb energy without appreciable leakage.

8. It is recommended that the design of boats of this type be based on the general procedure suggested in this report until a more rational design can be evolved.

9. It is recommended that for each type of design, model tests be conducted in a tank equipped with a wavemaker in order to determine the rigid-body motion of the vessel and to indicate the longitudinal load distribution on the bottom.

10. Further full-scale trials of the type discussed in this report are recommended in order to give more extensive data on the forces acting on planing craft. It would be especially informative to get quantitative data of the longitudinal load distribution over the hull girder, and to determine the variation of the impact factor with different angle of dead rise.

#### PERSONNEL

Arrangements for operation of the YP110 were made by F. Hawkins. The installation of the equipment and the conduct of the field tests were directed by E.L. Cecil, Jr. Mr. Cecil also made most of the detailed

---

\*Cf. Figure 18 of TMB Report 481 (Reference 4).

analyses of the measured data. Much effort was contributed by C.L. Pittiglio in connection with the installation and preparation of pressure and strain gages. Miss E. Adams derived the equations for the response of a damped single-degree-of-freedom system to a modified blast pulse. Electronic equipment was supplied and operated by personnel of the Applied Physics Laboratory. The investigation was made under the direction of the author.

#### APPENDIX

##### TRANSVERSE-LOAD DISTRIBUTIONS ON YP110

The instantaneous transverse-load distribution has been plotted for the impact which gave the highest pressure recorded for each gage on Frames 17, 23, and 26. For several other severe shocks the pressure distribution has been plotted for the several instants at which each of the gages in the particular transverse section reached a maximum; see Figures 13, 14, and 15.

#### ACKNOWLEDGEMENT

The information presented in this report was made possible by the excellent cooperation received from Mr. O.H. Oakley of the Bureau of Ships, Code 421. The idea of applying load factors to the design of PT boat structures, which has been used in this report, was first suggested by Mr. Oakley in a Bureau of Ships Memorandum, Code 420, dated 4 May 1948.

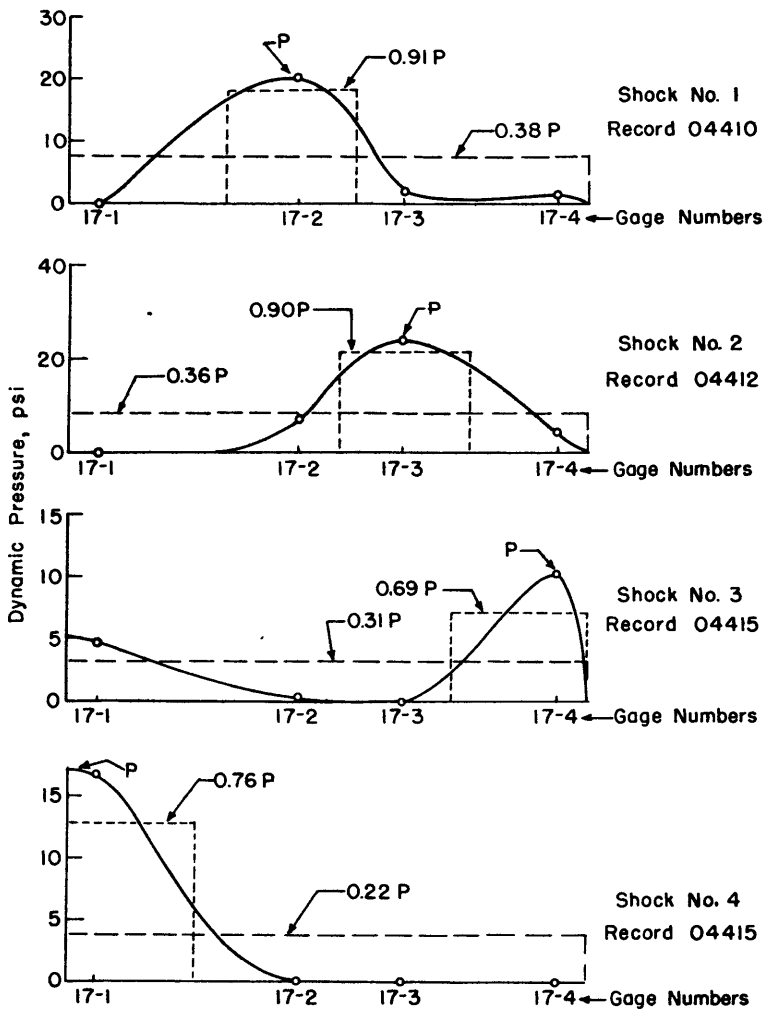


Figure 13a - Transverse Pressure Distribution at Instant of Maximum Pressure at Gages 17-1, 17-2, 17-3, and 17-4

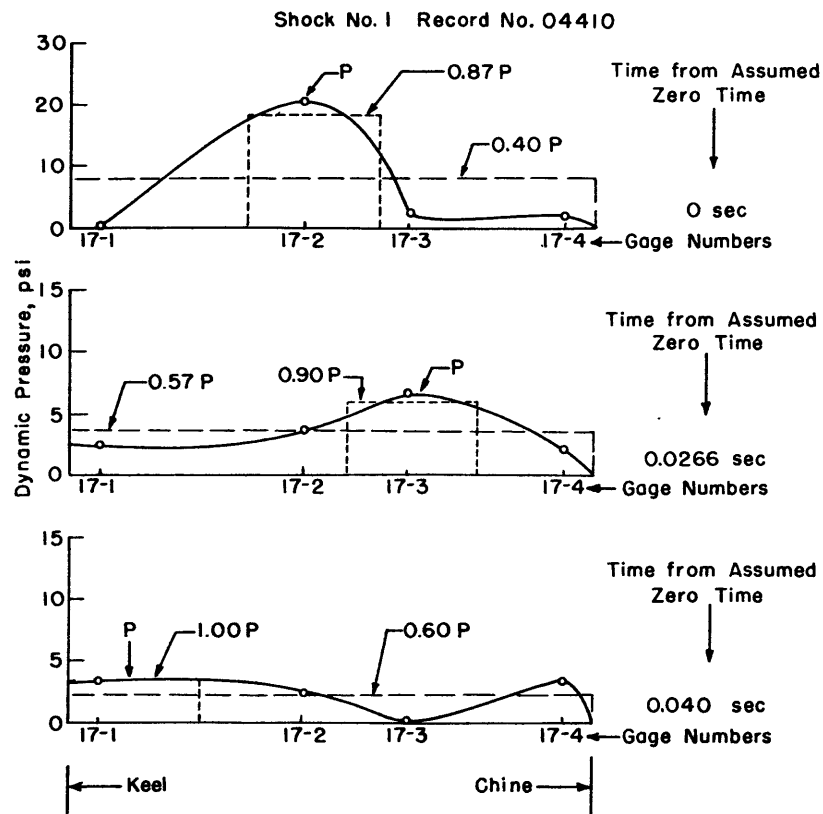


Figure 13b - Transverse Pressure Distribution at Instants during Shock 1 When Peak Pressure Was Recorded by Each Gage Peak



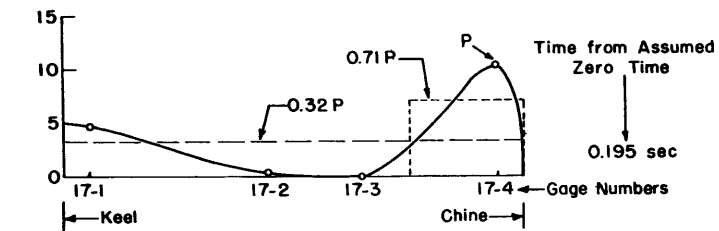
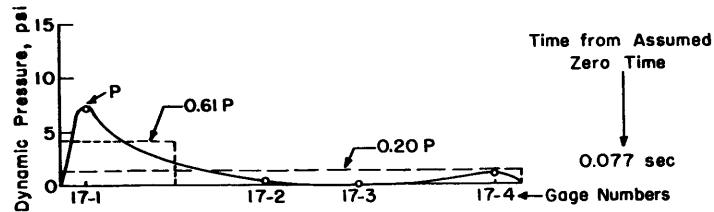
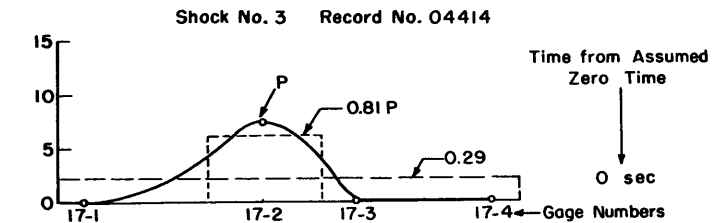
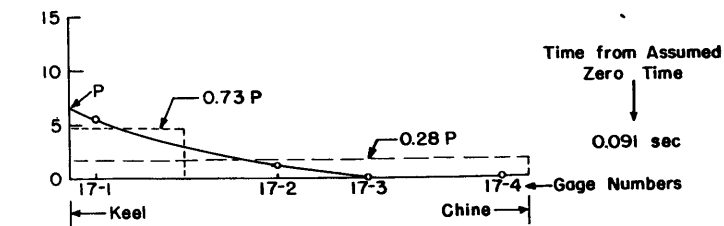
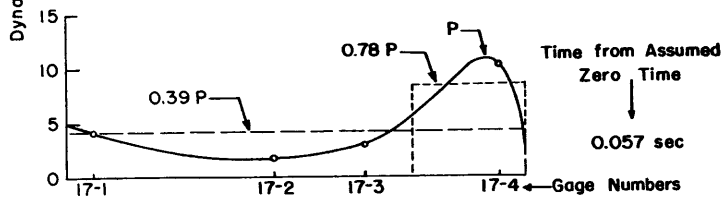
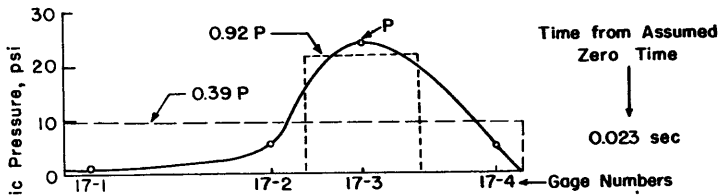
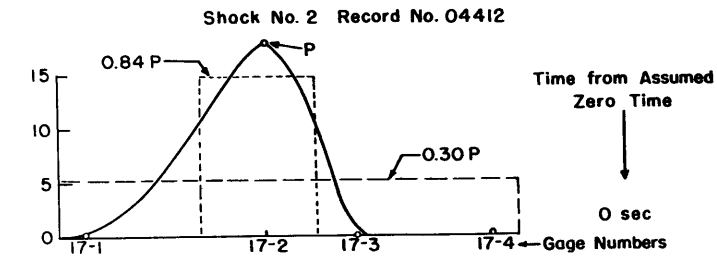
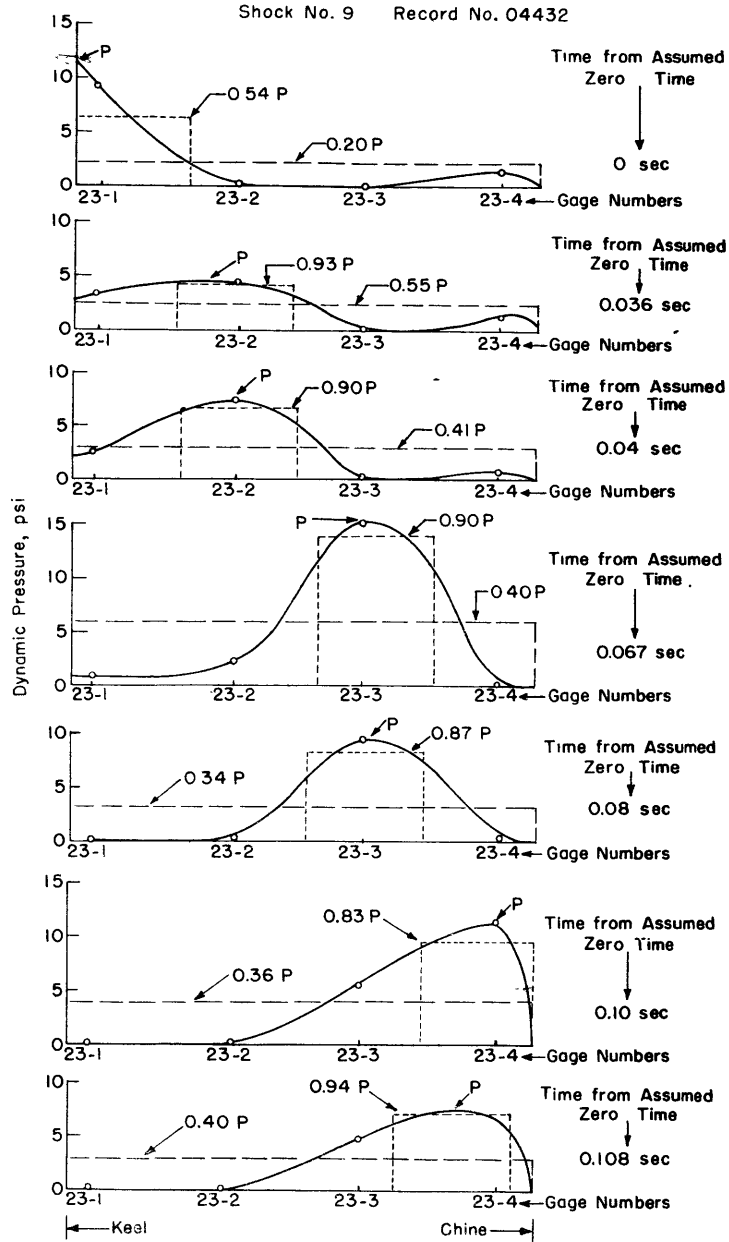


Figure 13c - Transverse Pressure Distribution at Instants during Shock 2 When Peak Pressure Was Recorded by Each Gage

Figure 13d - Transverse Pressure Distribution at Instants during Shock 3 When Peak Pressure Was Recorded by Each Gage

Figure 13 - Transverse Pressure Distributions at Frame 17 1/2



← Figure 14a - Transverse Pressure Distribution at Instants during Shock 9 When Peak Pressure Was Recorded by Each Gage

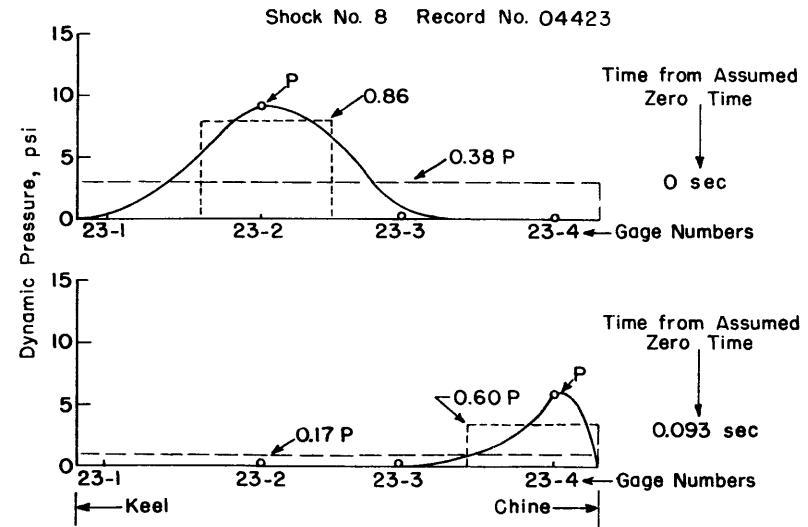


Figure 14b - Transverse Pressure Distribution at Instants during Shock 8 When Peak Pressure Was Recorded by Each Gage

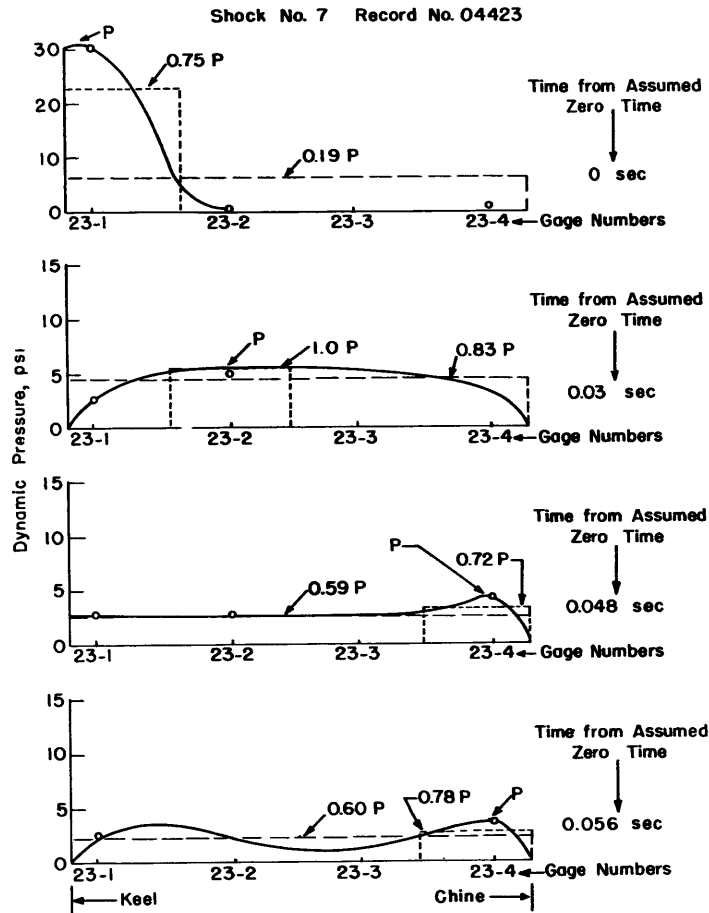


Figure 14c - Transverse Pressure Distribution at Instants during Shock 7 When Peak Pressure Was Recorded by Each Gage

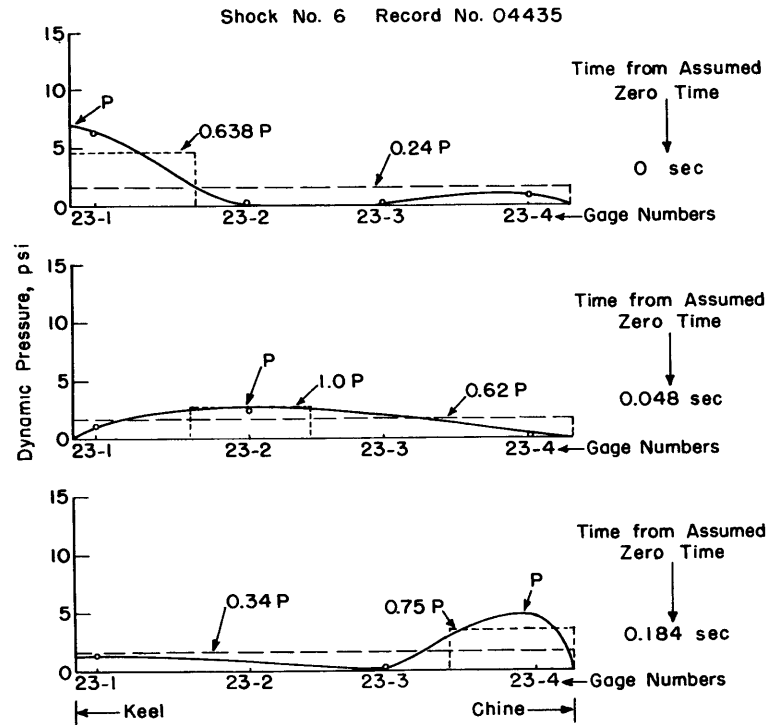


Figure 14d - Transverse Pressure Distribution at Instants during Shock 6 When Peak Pressure Was Recorded by Each Gage

Figure 14 - Transverse Pressure Distributions at Frame 23 1/2

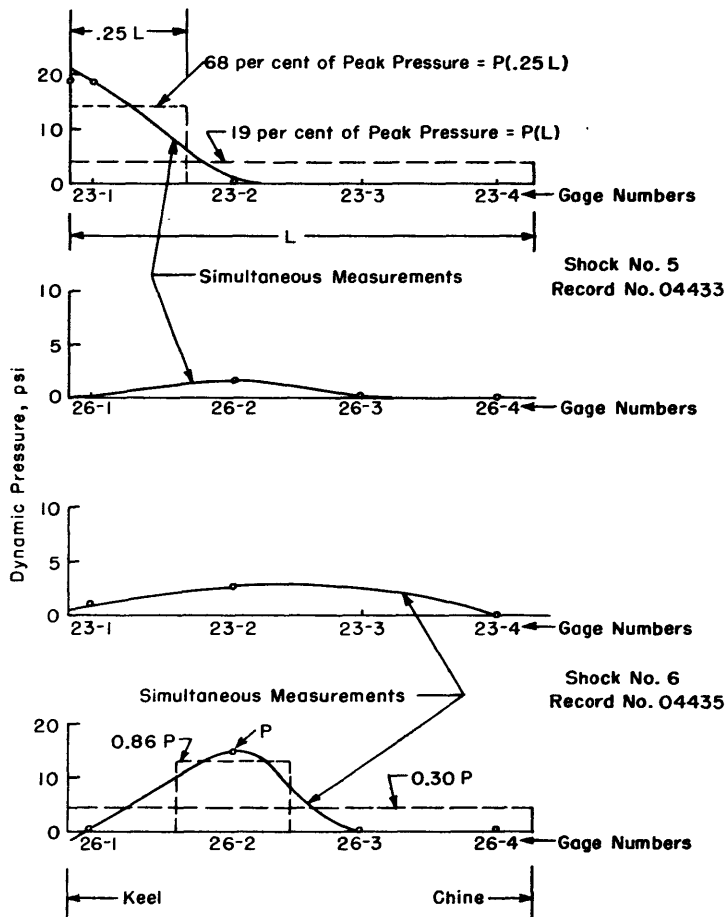


Figure 15a - Transverse Pressure Distribution at the Instant of Maximum Pressure at Gages 23-1 and 26-2

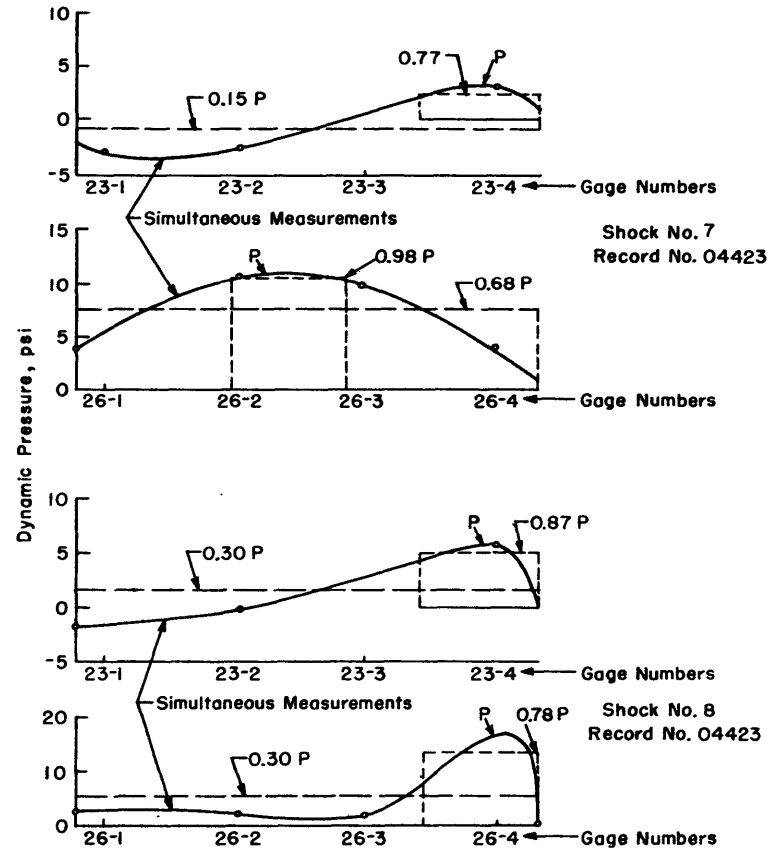


Figure 15b - Transverse Pressure Distribution at the Instant of Maximum Pressure at Gages 26-3 and 26-4

Figure 15 - Transverse Pressure Distributions at Frame 26 1/2

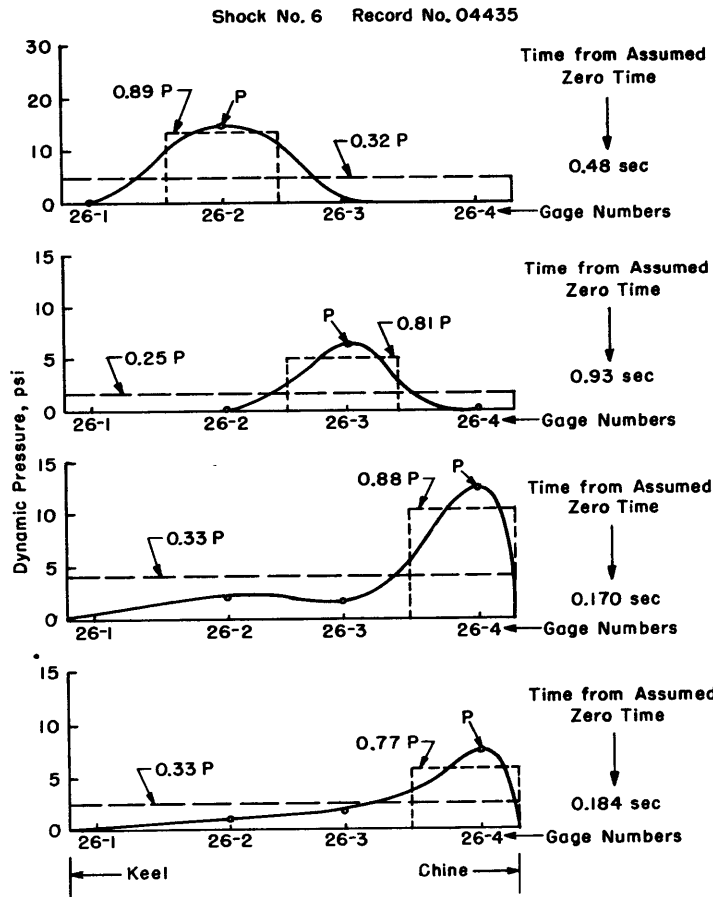


Figure 15c - Transverse Pressure Distribution at Instants during Shock 6 When Peak Pressure Was Recorded by Each Gage

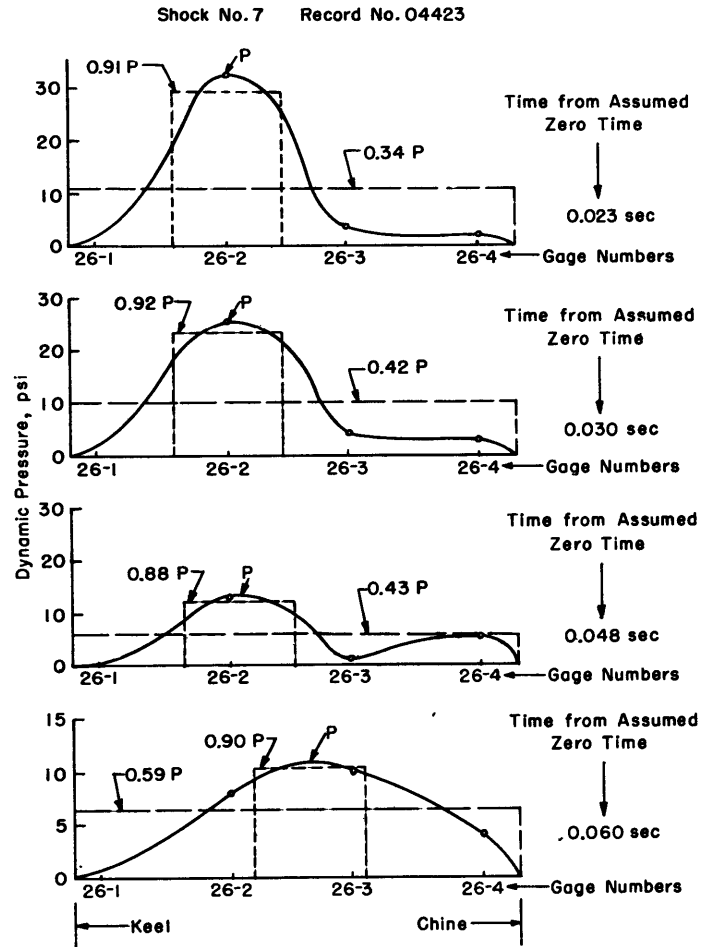


Figure 15d - Transverse Pressure Distribution at Instants during Shock 7 When Peak Pressure Was Recorded by Each Gage

Figure 15f - Transverse Pressure Distribution at Instants during Shock 9 When Peak Pressures Were Recorded by Each Gage

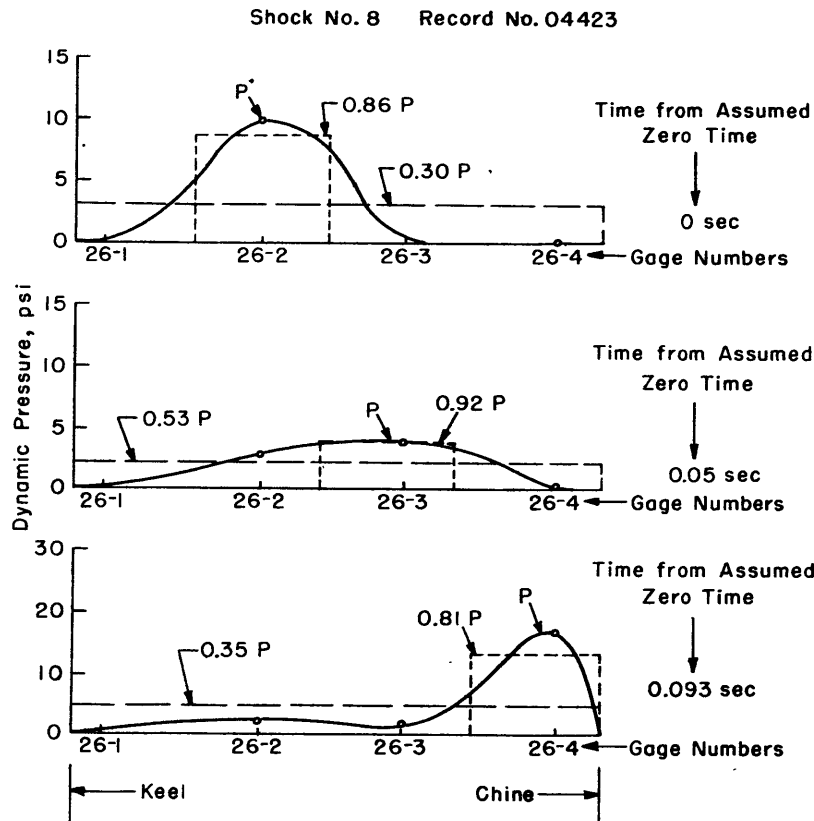
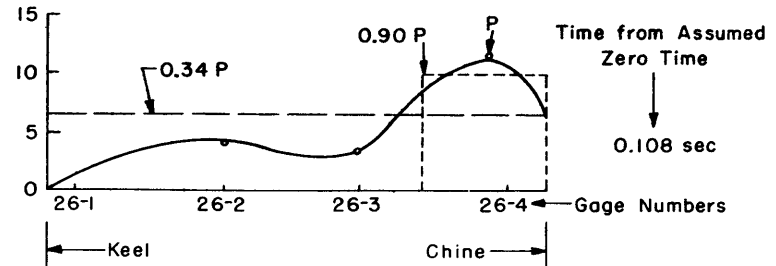
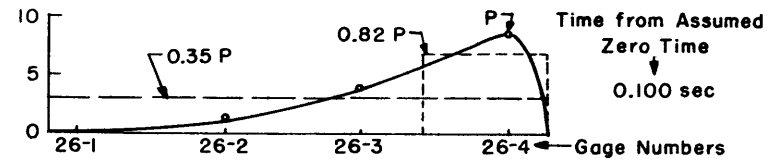
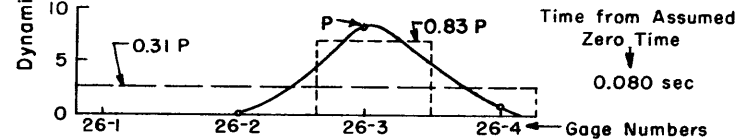
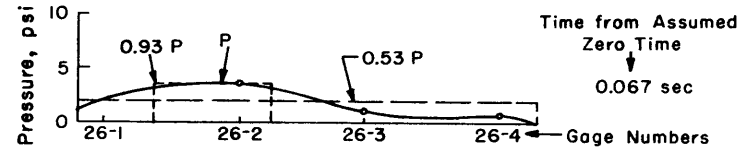
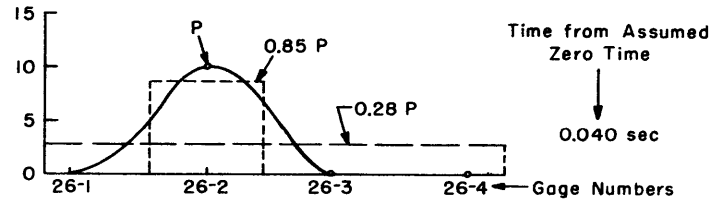
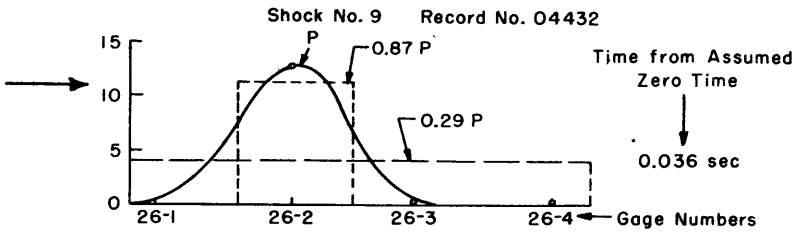


Figure 15e - Transverse Pressure Distribution at Instants during Shock 8 When Peak Pressures Were Recorded by Each Gage

REFERENCES

- (1) Bureau of Ships letter PT-8, PT/S1-2(422) of 21 January 1946 to TMB.
- (2) Cecil, E.L., Jr., "Impact Loads on the Hull of YP110 (Ex PT8) during Rough-Water Trials," TMB CONFIDENTIAL Report C-96, March 1948.
- (3) von Kármán, Th., "The Impact of Seaplane Floats during Landing," NACA Technical Note 321, 1929.
- ✓ (4) Frankland, J.M., "Effect of Impact on Simple Elastic Structures," TMB Report 481, April 1942. *Causey*
- (5) Robinson, Q.R., "The Jacklin Six-Component Recording Accelerometer and Its Performance," TMB Report 614, May 1948.
- (6) Wenk, Edward, Jr., "A Diaphragm-Type Gage for Measuring Low Pressures in Fluids," TMB Report 665, in preparation.
- (7) Cook, George W., "A Carrier-Type Strain Indicator," TMB Report 565, November 1946.
- (8) Siler, W.M., of Sparkman and Stephens, Inc., and Anderson of Anderson Fluke Engineering Co., "Impact Test Report of VEE-Bottom PT Boats 809-812," CONFIDENTIAL Report for Bath Iron Works, September 22, 1947.
- (9) BuAer Specifications NAVAER SS-1C-2, Airplane Strength and Rigidity, dated 12 June 1947.
- ✓ (10) Sydow, J., "A Comparison between Test and Calculation of the Hydrodynamic Forces Acting on the Bottom of Flying Boats during Take-Off and Landing," German Report No. 1592, Reference 23 of NavTechMisEu Technical Report 410-45, September 1945.





MIT LIBRARIES



3 9080 02753 9615

CONFIDENTIAL

AUG 7 1981

CONFIDENTIAL